J. Mol. Biol. (1993) **234**, 975–987

Genomic Footprinting of the Promoter Regions of *STE2* and *STE3* genes in the Yeast *Saccharomyces cerevisiae*

Brigitte Ganter, Song Tan and Timothy J. Richmond

Institut für Molekularbiologie und Biophysik
ETH-Hönggerberg, CH-8093 Zürich, Switzerland

(Received 31 May 1993; accepted 29 July 1993)

Dimethyl sulfate, DNase I and micrococcal nuclease DNA cleavage were combined with the ligation-mediated polymerase chain reaction to obtain high resolution maps of the promoter regions for two cell-type-specific genes: the **a**-specific *STE2* gene and the α-specific *STE3* gene. We find that MCM1 binds *in vivo* in **a**-cells to a 16 bp P-box sequence located in the *STE2* UAS. In α-cells, the footprint pattern is extended relative to **a**-cells, consistent with the additional binding of MATα2 to the sequences flanking each end of the P-box. A nucleosome was found adjacent to the P-box of the transcriptionally repressed **a**-specific *STE2* UAS in α-cells, positioned so that the nucleosome overlaps the TATA-box. In contrast, such well-positioned nucleosomes were not found for the transcriptionally active *STE2* UAS in **a**-cells, where instead the TATA box appears to be bound to the general transcription factor TFIID. These observations support the hypothesis that MATα2 repression of **a**-specific genes is mediated by nucleosomes, perhaps by exclusion of TFIID from the TATA-box.

Keywords: genomic footprinting; *STE2* and *STE3* genes; MCM1, MATα2 and MATα1; positioned nucleosomes

1. Introduction

The budding yeast *Saccharomyces cerevisiae* displays three differentiated cell types: the haploid **a** and α-mating types, which are specialized for mating with each other, and the diploid **a**/α cell type which is the fusion product of the two haploid cells. Cell-type specific gene expression is determined by the allele, *MAT*α or *MAT***a**, that occupies the mating-type locus (Strathern *et al.*, 1981). The three protein products, MATα1, MATα2, and MAT**a**1 expressed from the *MAT* locus are regulators of transcription (Sprague *et al.*, 1983; Johnson & Herskowitz, 1985). These cell type specific factors act in conjunction with several other regulatory proteins, so far identified as MCM1, STE12, SSN6 and TUP1, to account for cell-type-specific patterns of gene expression.

The protein MCM1, which is homologous to the mammalian serum response factor (SRF†) (Norman *et al.*, 1988), activates transcription of both **a** and α-specific genes (Passmore *et al.*, 1989; Elble & Tye, 1991). Although MCM1 shows similar affinity for both **a** and α-cell-specific upstream activating sequences (UAS) in *in vitro* experiments using purified proteins (Tan *et al.*, 1988), it activates only **a**-specific genes in **a**-cells and α-specific genes in α-cells. Further *in vitro* experiments showed that MCM1 binding to **a**-specific, but not to α-specific, UAS elements causes a conformational change in the protein, and this change was suggested to play a fundamental role in activation in **a**-cells (Tan & Richmond, 1990). The presence of MATα1 and MATα2 appears to account for the reversal of these gene activities in α-cells (Herskowitz, 1988, 1989; Sprague, 1990). In contrast to the results using purified proteins, experiments with crude extracts and synthetic oligonucleotides of the **a**-specific *STE2* UAS and the α-specific *STE3* UAS demonstrated that MCM1 binds specifically to the *STE2* UAS on its own, but binds to the *STE3* UAS only in the presence of MATα1 (Bender & Sprague, 1987, Bruhn *et al.*, 1992).

The consensus binding sites in the gene-specific UAS elements are well characterized. The 31 bp **a**-specific *STE2* UAS contains a central 16 bp pseudosymmetric P-box for MCM1 binding, flanked on

† Abbreviations used: SRF, serum response factor; UAS, upstream activating sequences; PRE, pheromone response element; DMS, dimethyl sulfate; LMPCR, ligation-mediated polymerase chain reaction.

0022-2836/93/240975-13 $08.00/0

either side by sequences for MATα2 binding (Johnson & Herskowitz, 1985; Keleher *et al.*, 1988). The α-specific *STE3* UAS contains a degenerate P-box (P'-box) and an adjacent Q-box that facilitates MATα1 binding (Jarvis *et al.*, 1988). In addition, a conserved repetitive element has been found upstream of pheromone inducible genes, such as *STE2*. This pheromone response element (PRE) mediates pheromone stimulation of transcription (Kronstad *et al.*, 1987; Van Arsdell *et al.*, 1987). The factor STE12 appears to bind very poorly to these DNA sequences on its own, but binds strongly and co-operatively when present together with MCM1 (Dolan *et al.*, 1989; Errede & Ammerer, 1989; Hwang-Shum *et al.*, 1991).

Recently, it has been shown that in addition to MATα2 and MCM1, two other non-cell-type specific proteins, SSN6 and TUP1, are also required for full repression of **a**-specific genes in α-cells (Keleher *et al.*, 1992). α-Cells harboring a mutation in the *ssn6* gene can mate at low efficiency to α-cells (Carlson *et al.*, 1984), and can express **a**-specific genes (Schultz & Carlson, 1987). A direct role for SSN6 in repression mediated by MATα2 is suggested by the reduced ability of MATα2 to repress transcription in *ssn6* mutants, and the ability of SSN6, when bound to DNA *via* a heterologous DNA-binding domain, to act as a transcriptional repressor (Keleher *et al.*, 1992).

Positioned nucleosomes can contribute critically to the regulation of transcription (Straka & Hörz, 1991; for reviews, see Simpson, 1991; Hayes & Wolffe, 1992), and thus the ability of **a**-specific UAS elements to act at a distance from the initiation site suggests that chromatin structure may be involved in the repression of **a**-specific gene expression by MATα2/MCM1. Nucleosome positioning has been shown to affect the function of a *cis*-acting element involved in the replication of yeast TRP1/ARS1 plasmids *in vivo* (Simpson, 1990), and evidence from the *STE6* UAS suggests that positioning of nucleosomes can be intimately involved in gene regulation (Shimizu *et al.*, 1991).

To complement our previous *in vitro* studies, we have performed *in vivo* footprint analyses of the **a**-specific *STE2* and the α-specific *STE3* UAS elements at nucleotide resolution using a modified protocol for the ligation-mediated polymerase chain reaction described originally by Mueller & Wold (1989) and optimized for *S. cerevisiae*. We have employed three different probes to examine the protein-DNA interactions in the cell: DMS methylation, micrococcal nuclease and DNase I. These experiments allow us to analyze the chromatin structure, including both nucleosomes and specific transcription factors, in the promoter regions. We find stably positioned nucleosomes in the promoter region of the **a**-specific *STE2* gene in α-cells, where this gene is repressed due to the presence of both MCM1 and MATα2. This array of stably positioned nucleosomes is not found in the transcriptionally active *STE2* gene in α-cells, where only MCM1 binds to the UAS element.

2. Materials and Methods

(a) *Yeast strains, plasmids and oligonucleotides*

Isogenic haploid strains BJ5458 (MATα, ura3-52, trp1, lys2.801. leu2Δ1, his3Δ200, pep4 :: HIS3, prblΔ1.6R, can1, GAL) and BJ5459 (MAT**a**, ura3-52, trp1, lys2.801, leu2Δ1, his3Δ200, pep4 :: HIS3, prblΔ1.6R, can1, GAL) (Jones, 1991) of *Saccharomyces cerevisiae* were obtained from the yeast genetic stock center (University of California, Berkeley). The following primers were used for the ligation-mediated PCR:
STE2 UAS coding strand primers:
(A1) 5'-CAGGCCAACGTCCATACTGCTTAGG-3';
(A2) 5'-CTGCTTAGGACCTGTGCCTGGCAAG-3';
(A3) 5'-CTGTGCCTGGCAAGTCGCAGATTGAAG-3';
STE2 UAS non-coding strand primers:
(B1) 5'-GTATTGCTTTGAAGTCAAATAAGATAC-3';
(B2) 5'-ATAAGATACTAATAGCACTCCTTAAATAG-3';
(B3) 5'-AGCACTCCTTAAATAGTATTCCACCCACAG-3';
(C1) 5'-ATCCATTCCCATATATGGAAGTGTAG-3';
(C2) 5'-AGTGTAGTTAATGGTGCTTTGACCAGG-3';
(C3) 5'-GGTGCTTTGACCAGGATTATACGTTGGATC-3';
STE3 UAS coding strand primers:
(D1) 5'-ATTGTACCACATTGCCAGATTTATGAAC-3';
(D2) 5'-GATTTATGAACTCTGGGTATGGGGTGC-3';
(D3) 5'-CTCTGGGTATGGGGTGCTAATTTTCGTTAG-3';
STE3 UAS non-coding strand primers:
(E1) 5'-AGAACTCTGCCTCTCCGTGATAACGG-3';
(E2) 5'-CTCTCCGTGATAACGGCCAAATGAAACGC-3';
(E3) 5'-GCCACTATACAATTTATTGTTTTCC-3'.
The following primers were used for the amplification of the specific labeled DNA-fragments, for the indirect end-labeling experiments: for *STE2*:
(1) PCRP#7: 5'-TCGACGGGTTCAACTTCTCC-3';
(2) PCRP#8: 5'-ACCTATATCCTAGAAGGAAG-3';
and for *STE3*:
(1) PCRP#3: 5'-AACGTTTTCTCCTTCTTTAC-3';
(2) PCRP#4: 5'-AGCAACGAATGGTTGTTTTATG-3'.
The blunt-end amplified PCR fragments were subcloned into the *Eco*RV site of pST14 (pUC9-derivative with a different multiple cloning site); pST14-*STE2* (pBG7) and pST14-*STE3* (pBG8). For the *in vitro* footprint analyses of the *STE2* UAS, the following oligonucleotides were annealed and subcloned into the *Sma*I site of pUC19:
STO4: 5'-CGCAGATTGAAGTCAACCATGTAAATTTCC-TAATTGGGTAAGTACATGATGAAACACATATGAA-GAAATT-3'; and
STO5: 5'-AATTTCTTCATATGTGTTTCATCATGTACT-TACCCAATTAGGAAATTTACATGGTTGACTTCAAT-CTGCG-3'.

The 70 bp *STE2* DNA contains the coding and the non-coding sequences from bases −179 to −234 (Hartig *et al.*, 1986; Nakayama *et al.*, 1985; Burkholder & Hartwell, 1985). For the *in vitro* footprint analyses of the *STE3* UAS, the 134 bp *Hae*II-*Hae*III fragment containing the coding and the non-coding sequences from bases −228 to −357 of the *STE3* element (Nakayama *et al.*, 1985) was used. This fragment was end-filled using Klenow enzyme (Boehringer-Mannheim) and subcloned into the *Sma*I site of pUC19 (pUC19-*STE3*). All the plasmid constructions, pUC19-*STE3*, pBG6 (pUC19-*STE2*), pBG7 (pST14-*STE2*) and pBG8 (pST14-*STE3*), were verified by the dideoxy sequencing method (Sanger *et al.*, 1977). All the oligonucleotides were synthesized on the 380B DNA Synthesizer (Applied Biosystems).

Standard techniques were employed for manipulation of DNA (Sambrook *et al.*, 1989). Oligonucleotides were 5' end-labeled with [γ-^{32}P]ATP using bacteriophage T4 polynucleotide kinase (New England Biolabs). The *STE2*

DNA, a 109 bp *Pst*I-*Eco*RI fragment of pBG6 (pUC19-*STE2*), was isolated by gel purification. The fragment was selectively 3′ end-labeled at the *Eco*RI site by end-filling with [α-^{32}P]dATP and Klenow enzyme, and at the *Pst*I site with [α-^{32}P]dCTP and T4 DNA polymerase (New England Biolabs). The 203 bp *Eco*RI-*Xho*I fragment of pBG7 and the 212 bp *Eco*RI-*Xho*I fragment of pBG8 were used to map the *STE2* UAS and *STE3* UAS, respectively by indirect end-labeling. A total of 30 to 60 ng of these purified fragments were labeled using the random primer method with [α-^{32}P]dCTP (400 Ci/mmol; Amersham) and Klenow enzyme (Feinberg & Vogelstein, 1983). Unincorporated nucleotides were separated from labeled DNA by gel filtration through Sephadex G-25.

(b) *Indirect end-labeling*

Chromosomal DNA (10 μg) prepared as described below was digested to completion with *Hin*cII (*STE2* UAS) or *Sal*I (*STE3* UAS) (New England Biolabs) in 50 μl of appropriate buffer. The digestion was stopped by the addition of 2 μl of 0·5 M EDTA and the DNA was precipitated with ethanol. The DNA was dissolved in 15 μl of 1 × loading buffer (0·04% (w/v) bromophenol blue, 0·04% (w/v) xylene cyanol, 5% (v/v) glycerol, 10 mM EDTA). The DNA samples were electrophoresed on a 1% agarose gel (10·5 × 25 cm) in 1 × TBE buffer (89 mM Tris·HCl, 89 mM boric acid, 2·5 mM EDTA) at 40 V for 16 h at room temperature. Control samples were treated identically.

The marker lane represents a partial *Eco*RI digest of a plasmid that contains 10 tandemly repeated 256 bp long DNA fragments of a 5 S ribosomal RNA gene (Thoma *et al.*, 1984, gift from F. Thoma). Following electrophoresis of DNA samples, transfer to nylon membranes (Zeta-Probe; Bio-Rad) was carried out by the alkaline Southern blotting method (Bio-Rad Bulletin 1233). Prehybridization, hybridization with DNA probes, and washing of membranes was carried out as described by Church & Gilbert (1984), with some modification as described by the manufacturer (Bio-Rad). In most cases, the membranes were exposed to film between intensifying screens at −70°C for 2 to 5 days (Ausubel *et al.*, 1987).

(c) *Cleavage of genomic DNA using dimethyl sulfate*

BJ5458 and BJ5459-cells were cultivated at 30°C to an A_{600} of 0·5 (5×10^7 cells/ml) in YPD medium (1% (w/v) yeast extract (BBL), 2% (w/v) Bacto-peptone (Difco) and 2% (w/v) dextrose (Merck)). The culture was harvested by centrifugation and resuspended in fresh YPD to 2×10^9 cells/ml, and then kept at room temperature for 5 min. After chilling the cells to 0°C, DMS was added to a final concentration of 0·2% in each sample. Cells were incubated for times ranging from 5 to 20 min, and then methylation was terminated by 20-fold dilution in 20 mM Tris·HCl (pH 8·0), 20 mM sodium azide. Cells were converted to spheroplasts at 30°C using zymolyase (Chemie Brunschwig). The spheroplasts were lysed by addition of an equal volume of 50 mM Tris·HCl (pH 7·4), 1 M NaCl, 2% (w/v) SDS, 50 mM EDTA to the suspension. To obtain protein-free DNA, the lysed spheroplasts were extracted with 25 : 24 : 1 phenol : chloroform : isoamylalcohol, and 24 : 1 chloroform : isoamylalcohol, and then treated with RNase A, re-extracted and precipitated. The *STE2* and *STE3* DNA were purified and digested with *Hin*cII and *Hin*dIII, respectively. The DNA was dissolved in freshly prepared 1 M piperidine and cleaved at methylated guanine residues by incubation at 90°C for 30 min, and then precipitated and lyophilized several times from water (twice) and 50% ethanol (twice). Naked DNA was prepared as above from unmethylated yeast cells, digested with the appropriate restriction enzyme, and dissolved in 50 mM sodium cacodylate (pH 8), 1 mM EDTA. This DNA was reacted with 0.2% DMS at room temperature for 6 min, precipitated with ethanol, and hydrolyzed using the G-specific reaction of Maxam & Gilbert (1980).

(d) *Digestion of genomic DNA using DNase I and micrococcal nuclease*

The BJ5458 and BJ5459-cells were grown and harvested as described above. Cells were converted to spheroplasts at 30°C using the enzyme zymolyase. For the genomic footprinting with DNase I, spheroplasts were resuspended to a density of 7×10^9 spheroplasts/ml in 100 mM NaCl, 10 mM Tris·HCl (pH 7·4), 10 mM $MgCl_2$, 5 mM β-mercaptoethanol and 0·075% (v/v) Nonidet P-40. DNase I (Sigma) was added to 20 to 50 Kunitz units/3 ml and the reaction was incubated at 20°C for 5 min. Digestions were terminated by the addition of an equal volume of 50 mM Tris·HCl (pH 7·4), 1 M NaCl, 2% SDS and 50 mM EDTA. Genomic DNA was isolated as described above. Purified naked DNA was dissolved in 0·1 mM EDTA, 10 mM Tris·HCl (pH 8) and digested in 40 mM Hepes (pH 7·5), 20 mM $MgCl_2$, 5 mM $CaCl_2$ using 0·5 to $2{\cdot}5 \times 10^{-5}$ units DNase I/μg DNA. Digestions were carried out for 5 min at 37°C and terminated by the addition of EDTA to 10 mM.

For footprinting with micrococcal nuclease (MNase), the spheroplasts were resuspended in 150 mM NaCl, 20 mM Tris·HCl (pH 8), 5 mM KCl, 1 mM EDTA, 5 mM β-mercaptoethanol, 5 mM $CaCl_2$ and 0·075% (v/v) Nonidet NP-40 to a density of 7×10^9 spheroplasts/ml. MNase (Boehringer-Mannheim) was added to 50 to 150 units/3 ml, and the reaction mixture was incubated at 20°C for 5 min. Digestions were terminated as for the DNase I procedure, and genomic DNA was isolated. Naked DNA was digested in 20 mM Tris·HCl (pH 8), 150 mM NaCl, 5 mM KCl, 1 mM EDTA, 5 mM $CaCl_2$ using $1{\cdot}6 \times 10^{-3}$ to $1{\cdot}9 \times 10^{-2}$ units MNase/μg DNA. Before using this DNA for ligation-mediated polymerase chain reaction (LMPCR), 25 μg of purified chromosomal DNA was phosphorylated with T4 DNA polynucleotide kinase (New England Biolabs, 0·5 units per μg of DNA) in 75 μl of 1 × buffer (50 mM Tris·HCl pH 7·6, 10 mM $MgCl_2$, 5 mM DTT, 1 mM EDTA (pH 8·0)). After 1 hour of phosphorylation at 37°C, the enzyme was inactivated by incubating at 75°C for 10 min. This DNA was used directly for LMPCR.

For all digestions, 3 preparations from yeast cells were made, and in each case 4 different nuclease concentrations were used. Except for nucleosome maps, where 2 to 4 digestion conditions are shown, a single representive footprint is presented in the Figs.

(e) *DNA amplification by ligation-mediated PCR*

In step 1, a DNA primer is annealed to the cleaved genomic DNA and extended. A total of 1 μg of DMS-treated or 3 μg of DNase I or MNase-treated chromosomal DNA and 0·3 pmol of primer DNA were dissolved in 40 mM Tris·HCl (pH 7·5), 50 mM NaCl and 14 mM $MgCl_2$ to give a 14 μl total volume. The sample was denatured for 5 min at 95°C and then incubated for 30 min at a temperature dependent on the t_m ($t_m = 81{\cdot}5 + 16{\cdot}6(\log M) + 0{\cdot}41(\%GC) - 500/n$, where M is the molarity of the salt and n the length of the oligonucleotide

used; Wahl *et al.*, 1987) of the oligonucleotide in order to anneal the primer. After brief centrifugation to collect condensation, 16 μl of 16·6 mM DTT, 120 mM Tris·HCl (pH 7·9), 20 μM dNTP and 1 unit of T7 DNA polymerase (New England Biolabs) were added, and the reaction was incubated at 37 °C for 15 min. The extension reaction was stopped by incubation for 10 min at 65 °C and then transferred to an ice bath.

In step 2, double-stranded linker DNA is ligated to the extended template, and the resultant fragments are amplified by PCR (Mueller & Wold, 1989). The linker used was the same as the one described by Mueller & Wold (1989). A total of 20 μl of a solution containing 50 mM Tris·HCl (pH 7·6), 12·5 mM $MgCl_2$, 25 mM DTT, 1·25 mM rATP, 60 units of T4 DNA ligase (New England Biolabs), and 60 pmol of linker DNA was added to the extension reaction mixture and incubated overnight at 14 °C. The reaction was stopped by heating at 65 °C for 10 min. The sample was precipitated with ethanol in the presence of 10 μg of yeast carrier tRNA. The dried pellet was resuspended in 84 μl of H_2O, 10 μl of 166 mM $(NH_4)_2SO_4$, 677 mM Tris·HCl (pH 8·8), 67 mM $MgCl_2$, 100 mM β-mercaptoethanol and bovine serum albumin (BSA) was added to 0·17 mg/ml. To this solution were added 20 nmol of each of dNTP, 10 pmol of both amplification primers and 1 unit of Taq DNA polymerase (Cetus). The samples were covered with 90 μl of mineral oil, heated at 95 °C for 5 min and then amplified in a Cetus Thermal Cycler for 16 cycles. A cycle consists of denaturation for 1 min at 95 °C, hybridization for 2 min at 50 to 70 °C, where the exact temperature depends on the t_m (Wahl *et al.*, 1987) of the oligonucleotides used, and extension for 2 min at 76 °C with 5 s extension per cycle. After this 16 cycles an extension of 10 min at 76 °C was carried out.

In step 3, a radioactive DNA primer is annealed to the amplified DNA and extended. The primer DNA was labeled with T4 polynucleotide kinase as described above. A total of 5 μl of the labeling mixture containing 16·6 mM $(NH_4)_2SO_4$, 67·7 mM Tris·HCl (pH 8·8), 6·7 mM $MgCl_2$, 10 mM β-mercaptoethanol and 0·17 mg bovine serum albumin/ml were added, followed by 1·4 nmol of each dNTP, 0·5 to 1 pmol of labeled primer DNA and 1 unit of Taq DNA polymerase. Samples were heated at 95 °C for 5 min, hybridized at temperature between 60 to 70 °C, where the exact temperature depends on the t_m (Wahl *et al.*, 1987) of the oligonucleotide used, and extended for 5 min at 76 °C. This process was repeated twice, but with an incubation time at 95 °C of 1 min. Finally, an extension for 10 min at 76 °C was carried out. Polymerase activity was stopped by chilling on ice, adding 295 μl of 260 mM sodium acetate, 10 mM Tris·HCl (pH 7·5), 4 mM EDTA, and then the DNA was purified by extraction with phenol and 24 : 1 chloroform : isoamyl alcohol. The samples were precipitated, resuspended in 0·25% (w/v) bromophenol blue, 0·25% (w/v) xylene cyanol, 0·03% (v/v) glycerol, 60 mM EDTA (to 1000 to 5000 cpm/μl), and 4 μl of each sample was loaded onto a 6% sequencing gel (Sambrook *et al.*, 1989). The gel was transferred to 3 MM filter paper, dried and autoradiographed. The intensity of bands in the MNase footprint gels were measured with an Optronics P-1000HS densitometer set at 100 μm resolution using autoradiographs that were exposed without intensifying screens to a maximum absorbance less than 2.

(f) *DNase I and DMS protection assays* in vitro

The methods used are essentially as described by Treisman (1986) and include separating free DNA from protein-complexed DNA on band-shift gels. Binding reactions were carried out in a 20 μl final volume containing 20 mM sodium cacodylate (pH 8·0), 5·3 mM $MgCl_2$, 50 mM NaCl, 5% glycerol, end-labeled DNA fragment and protein sample. The binding mixture was incubated for 10 min at 4 °C before the sample was treated with DNase I. A total of 1 μl of 100 mM $CaCl_2$ and 1 μl (10^{-2} to 10^{-4} Kunitz units/μl) DNase I were added to the binding mixture, and the reaction was incubated for 90 s at 4 °C. The reaction was stopped by addition of 1 μl of 0·5 M EDTA and loaded onto a 5% polyacrylamide gel (40 : 1 acrylamide : bis-acrylamide) in 45 mM Tris·HCl, 45 mM boric acid and 1·25 mM EDTA. For the DMS protection assay, 1 μl of a 1 : 100 dilution of DMS in binding buffer was added to the binding mixture, and the reaction incubated at 4 °C for 15 to 21 min before the addition of 1 μl of 5 M β-mercaptoethanol and loading onto the gel. For all assays, the complexed DNA was separated from free DNA on a band shift gel. The wet gel wrapped in Saranwrap was autoradiographed for 1 to 3 h to locate the DNA fragments. The DNA bands were excised from the gel, eluted, and purified from the polyacrylamide matrix (Treisman, 1985). The samples were then fractionated on denaturing 6 or 8% polyacrylamide gels. Autoradiography was carried out at −70 °C using intensifying screens (Ausubel *et al.*, 1987).

3. Results

(a) *DMS and DNase I footprints of the* STE2 *P-box region in* **a** *and* α*-cells*

Nucleotide-resolution maps of the *STE2* UAS in chromatin were obtained using DMS and DNase I cleavage followed by ligation-mediated PCR. Guanine specific cleavage of naked chromosomal DNA provide size markers (see Fig. 9 for sequences). The DMS protection pattern from **a**-cells show that one coding strand G base at position −209 (Fig. 1(a), lane 3) and two G bases on the non-coding strand at positions −217 and −218 (Fig. 1(a), lane 6) within the P-box of the *STE2* UAS are protected from methylation indicating that MCM1 is binding to the *STE2* UAS in **a**-cells. In α-cells, the non-coding strand shows strongly protected sites at positions −202 and −229 (Fig. 1(a), lane 5). For the coding strand, an additional protection at position −226 is visible (Fig. 1(a), lane 2). This extended protection pattern flanking both sides of the P-box is consistent with MATα2 binding to its operator in α-cells, when compared to the *in vitro* methylation protection results seen for the ternary MCM1/MATα2/*STE2* complex (Fig. 2(a), lanes 3 and 6).

Although there are three G residues at positions −209 to −211 on the coding strand of the *STE2* UAS, only one is observed by DMS methylation of the genomic DNA (Fig. 1(a), lanes 1). We assume that the missing G residues are an artifact resulting from the ligation-mediated PCR procedure since all three G residues are found when this region is subcloned into a plasmid vector and sequenced by dideoxy termination (data not shown).

The DNase I cleavage patterns in the region of the P-box show a well-protected site on both

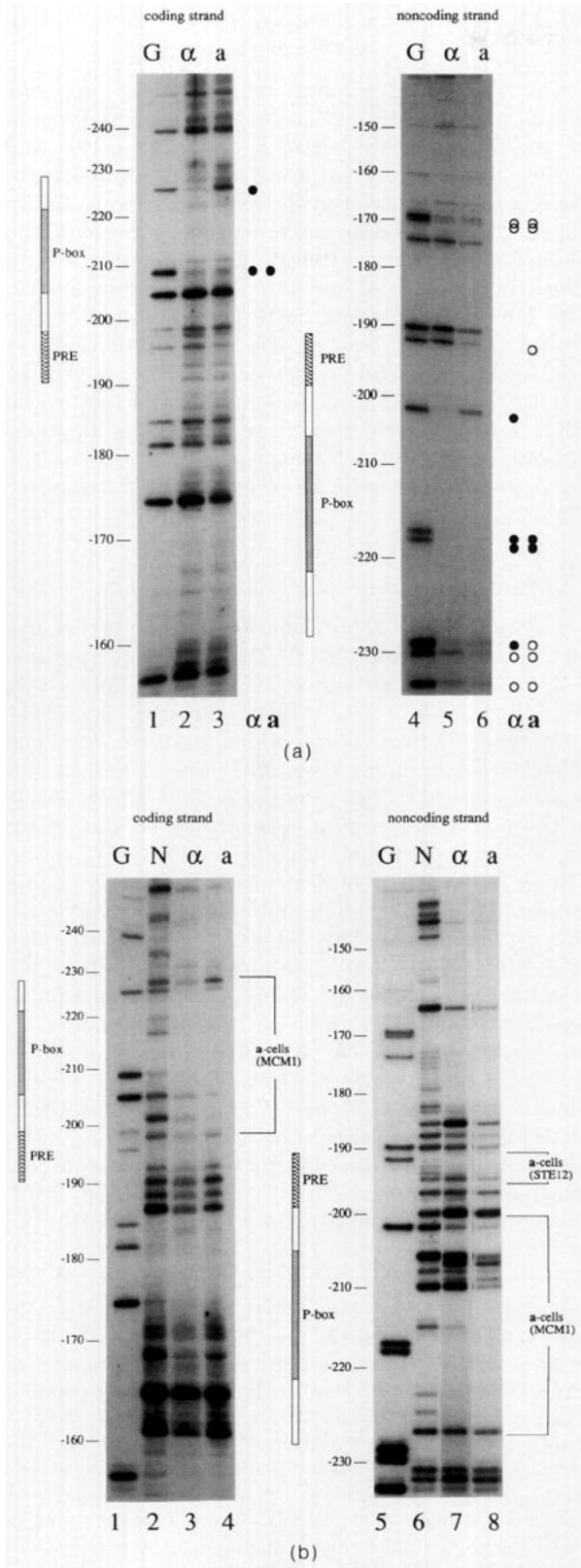

Figure 1. Genomic footprints of the **a**-specific *STE2* UAS in **a** and α-cells using the DMS reaction and DNase I cleavage. (a) The coding strand is shown in lanes 1 to 3, and the non-coding strand in lanes 4 to 6 using DMS treatment. Cleavage of the naked chromosomal DNA at G bases is shown in lanes 1 and 4 (G). Lanes 3 and 6 show the protection pattern of the *STE2* UAS in **a**-cells and lanes 2 and 5 show the protection pattern in α-cells. The regions covered by the P-box and PRE are indicated for each strand. (●) G bases strongly and (○) weakly protected are noted for both cell types in lanes α and **a**. (b) The coding strand is shown in lanes 1 to 4, and the non-coding strand in lanes 5 to 8 using DNase I. Cleavage of the naked chromosomal DNA at G residues is shown in lanes 1 and 5 (G). Limited digestion of the naked chromosomal DNA with DNase I is shown in lanes 2 and 6 (N). Lanes 4 and 8 show the protection pattern in **a**-cells, and lanes 3 and 7 show the protection pattern in α-cells. The protected regions in **a**-cells are indicated by square brackets. (a) and (b) The origin of the base-pair numbering is the initiation codon.

strands between position −199 and −227 in both cell types. Each footprint is interrupted by a hypersensitive cutting site at position −206 on the non-coding strand (Fig. 1(b), lanes 7 and 8, also Fig. 7). Although the same region is protected in **a**-cells and α-cells, there are variations in the two DNase I cutting patterns. The pattern for the region from bases −205 to −209 along the non-coding strand is significantly different for the naked DNA, the **a**-cell, and the α-cell samples (Fig. 1(b), lanes 6 to 8).

We compared these *in vivo* footprints to the *in vitro* patterns of the MCM1-*STE2* and MCM1-MATα2-*STE2* complexes. For the *in vitro* experiments, the free DNA was separated from the protein-DNA complex by gel electrophoresis after treatment with footprinting reagent and prior to analysis of the protection pattern. The DNase I digestion patterns of the MCM1-DNA complex (Fig. 2(b), lanes 3 and 7) show that the same region centered on the pseudodyad axis of the P-box is protected *in vitro* as *in vivo* for **a**-cells, and that the details of the patterns are highly similar. For example, the single hypersensitive cutting site at position −206 on the non-coding strand seen *in vivo* (Fig. 1(b), lane 8) is also present *in vitro* (Fig. 2(b), lane 7). In contrast, the DNase I digestion pattern of the ternary MCM1-MATα2-DNA complex shows substantial differences with the α-cell pattern *in vivo*. The *in vitro* pattern (Fig. 2(b), lanes 4 and 8) shows that the MATα2 binding site between position −192 and −232 extends in both directions beyond the region protected between position −199 and −226 by MCM1 alone, whereas the extent of protection *in vivo* was between position −199 and −227 in both **a** and α-cells.

The *in vitro* methylation protection results indicate that the two G bases at position −209 and −210 on the coding strand (Fig. 2(a), lane 2), and the two G bases at position −217 and −218 on the non-coding strand (Fig. 2(a), lane 5) are protected when MCM1 is bound alone. When MATα2 is added to the DNA binding mixture, the G base at position −226 on the coding strand and the G base at position −202 on the non-coding strand are also protected, consistent with the *in vivo* methylation results (Fig. 1(a), lane 5). These results are summarized in Figure 9.

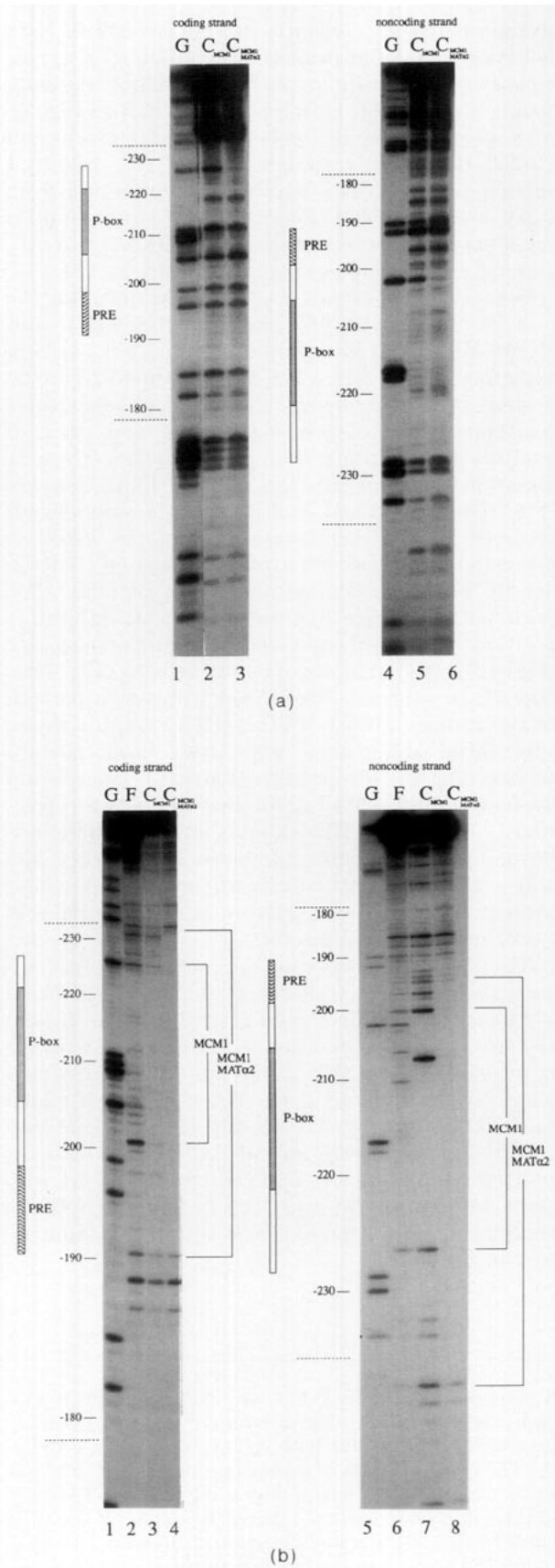

Figure 2. *In vitro* footprints of MCM1 and MCM1/MATα2-*STE2* UAS complexes using the DMS reaction and DNase I cleavage. (a) Lanes 1 to 3 show the coding strand, and lanes 4 to 6 show the non-coding strand of the 3′ end-labeled, 109 bp *Pst*I-*Eco*RI DNA-fragment treated with DMS. Cleavage of the free DNA at G bases is shown in lanes 1 and 4 (G). Lanes 2 and 5 show protection of the DNA to DMS methylation in the MCM1-*STE2* complex (C_{MCM1}), and that for the MCM1/MATα2-*STE2* complex ($C_{MCM1/MAT\alpha2}$) in lanes 3 and 6. (b) Lanes 1 to 4 show the coding strand and lanes 5 to 8 show the non-coding strand of the 109 bp 3′ end-labeled DNA-fragment treated with DNase I. Cleavage of the free DNA at G bases is shown in lanes 1 and 5 (G). Limited digestion of the free DNA separated from the MCM1 binding reaction with DNase I is shown in lanes 2 and 6 (F). The DNase I protection pattern of the MCM1-*STE2* complex (C_{MCM1}) is shown in lanes 3 and 7 and that for the MCM1/MATα2-*STE2* complex ($C_{MCM1/MAT\alpha2}$) in lanes 4 and 8. The DNA regions protected by bound protein are indicated by brackets. (a) and (b) The location of the P-box and PRE-box are shown and the limits of the *STE2* sequence are denoted (----). The bases are numbered as for Fig. 1.

(b) *DMS and DNase I footprints of the* STE2 *PRE in* **a** *and* α*-cells*

The *cis*-acting pheromone response element (PRE) binds the STE12 factor and spans the region of the *STE2* UAS between position −191 and −198, immediately adjacent to the downstream MATα2 binding site (Burkholder & Hartwell, 1985). When DMS is used as the footprinting reagent, the G base at position −192 of the non-coding strand (Fig. 1(a), lane 6) is partially protected in **a**-cells. The DNase I footprint pattern on the non-coding strand (Fig. 1(b), lane 8) also shows protection at position −193 and −194 within the PRE. In α-cells, where MATα2 is present, the G bases in the PRE are not protected from DMS modification, although the DNase I footprint appears to be the same in **a** and α-cells (Fig. 1(b), lane 7, also see Fig. 7).

(c) *DMS footprints of the* STE3 *UAS in* **a** *and* α*-cells*

In vivo DMS protection shows that two G residues on the coding strand of the *STE3* P′-box at positions −321 and −322 are protected in both **a** and α-cells (Fig. 3(a), lanes 1 to 3). This compares favorably with the *in vitro* protection pattern for the MCM1-DNA complex (Fig. 3(b), lanes 1 and 2) and is consistent with the hypothesis that MCM1 binds to the *STE3* P′-box in **a**-cells. However, data from the non-coding strand do not confirm this claim. The *in vitro* pattern of protection on the non-coding strand at position −329 and enhancement at position −331 for the MCM1-DNA binary complex (Fig. 3(b), lanes 4 and 5) is observed only in α-cells (Fig. 3(a), lanes 4 to 6). There is little protection at position −329 and little or no enhancement at position -331 in **a**-cells. (Fig. 3(b), lanes 4 and 6).

The *in vitro* DMS methylation studies of the binary MCM1-*STE3* and of the ternary MATα1-MCM1-*STE3* complexes show that there is no additional protection observed in the ternary complex relative to the binary complex (Fig. 3(b)). Protection occurs only in the P′-box and not in the

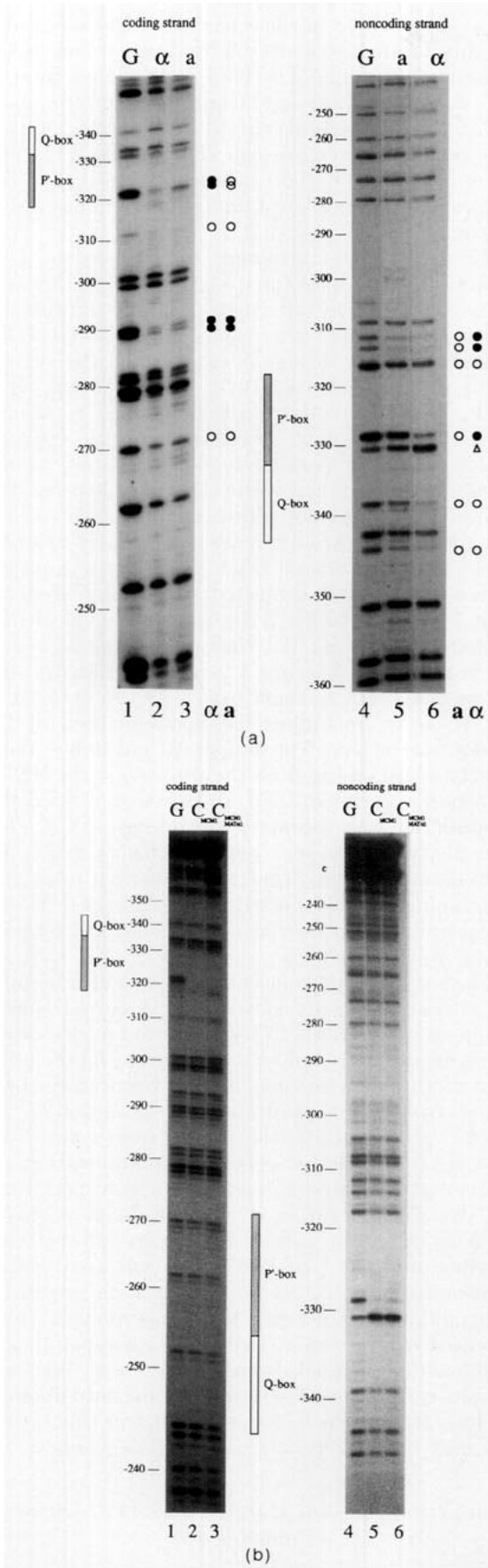

Figure 3. (a) Genomic footprints of the α-specific *STE3* UAS in **a** and α-cells using the DMS reaction. The coding strand is shown in lanes 1 to 3, the non-coding strand in lanes 4 to 6. Cleavage of the naked chromosomal DNA at G bases is shown in lanes 1 and 4 (G). Lanes 3 and 5 show the protection pattern found in **a**-cells and lanes 2 and 6 show the protection pattern in α-cells. The location of the P'-box and Q-box are also shown. (●) G bases strongly and (○) weakly protected or enhanced in cleavage (Δ) are noted for both cell types in lanes α and **a**. (b) *In vitro* footprints of MCM1 and MCM1/MATα1-*STE3* UAS complexes using the DMS reaction. Lanes 1 to 3 show the coding strand and lanes 4 to 6 show the noncoding strand of the 3′ end-labeled 170 bp DNA fragment. Cleavage of the free DNA at G bases is shown in lanes 1 and 4 (G). Lanes 2 and 5 show protection of the DNA to DMS methylation in the MCM1-*STE3* complex ($C_{MCM1/MAT\alpha1}$). The location of the P'-box and Q-box are also shown. (a) and (b) The origin of the base-pair numbering is the initiation codon.

Q-box nor in any adjacent region. In contrast, *in vivo* footprinting shows protection on the noncoding strand around the Q-box at bases −339 and −345 in both **a** and α-cells. Protection is also observed in both cell types on the coding strand around bases −310 and −290 and on the noncoding strand around base −315 (Fig. 3(a)). Additional factors not present in the *in vitro* studies may be binding to these sites *in vivo*. The footprinting results for the *STE3* UAS *in vivo* and *in vitro* experiments are summarized in Figure 9.

In addition to DMS, we attempted to map the *STE3* UAS with DNase I in both cell types, but obtained footprints identical with the naked DNA (results not shown). This result is probably due to rearrangement or degradation of the protein-DNA complex during the preparation of the cells before DNase I is introduced, which in comparison to the DMS method, requires more time.

(d) *MNase and DNase I maps of the* STE2 *UAS in* ***a*** *and α-cells*

The chromatin structure of the *STE2* promoter region was mapped in whole cell lysates at low resolution (±20 bp). Spheroplasts were generated from **a** and α-cells, lysed in a hypotonic buffer containing divalent cations, and subjected to mild digestion at room temperature with MNase. Indirect end-labeling of the genomic DNA reveals a cleavage pattern downstream of the α2 binding site in α-cells indicative of positioned nucleosomes (Fig. 4, lanes 2 and 3). The repeating hypersensitive sites spanning the promoter region have centers of cleavage approximately at positions −180, −34, and +124 relative to the transcription initiation site. These periodic regions of nuclease cutting at the spacings seen here are most simply interpreted as a series of stably positioned nucleosomes. No such repeating cutting pattern was found in **a**-cells, although the region around position −50, which contains the TATA-box was found to be hypersensitive to MNase digestion (Fig. 4, lanes 6 and 7).

These indirect end-labeling studies show that nucleosomes are well positioned on the *STE2* UAS in α-cells. However, such experiments are limited in

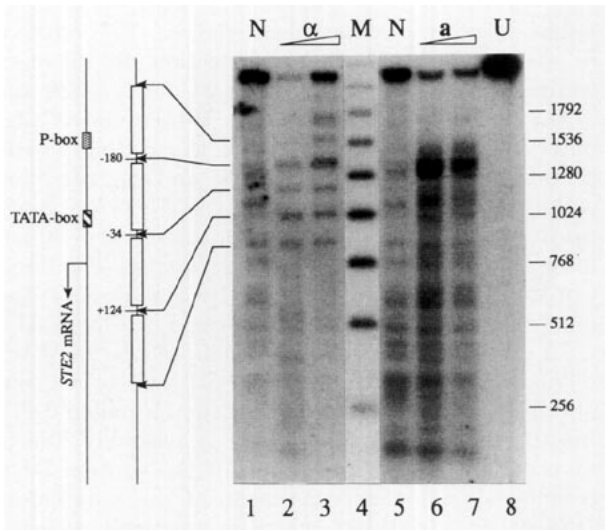

Figure 4. Genomic footprints of the *STE2* UAS and initiation site at low resolution in **a** and α-cells. Chromatin was cleaved with MNase in spheroplasts, followed by analysis of the *STE2* promoter using indirect end-labeling. For α-cells, digestion with 20 and 40 units enzyme/ml gives the pattern in lanes 2 and 3, and analogously for **a**-cells in lanes 6 and 7. A limited digestion of naked chromosomal DNA is shown in the lanes 1 and 5 (N). The marker DNA fragments are concatemers of 256 bp (see Materials and Methods) and are shown in lane 4 (M) with their lengths indicated along the right border. Undigested chromosomal DNA is shown in lane 8 (U). The boxes on the left represent the regions of chromatin protected as compared to the deproteinized DNA. The nuclease sensitive regions upstream of the *STE2* gene in α-cells are also indicated by the arrows.

resolution and offer no information regarding the structure of individual nucleosomes. To investigate protein-DNA interactions and chromatin structure at nucleotide-level resolution, we again used the ligation-mediated polymerase chain reaction in conjunction with MNase digestion. The region of the *STE2* UAS examined in whole cell lysates from **a** and α-cells extends from −231 to +36. A strongly protected region is apparent between bases −161 and −47 on the coding strand in α-cells (Fig. 5(a), lanes 3 and 4), and this result together with those from the low resolution mapping leads us to propose the presence of nucleosome I approximately centered at base-pair −116 or 96 bp downstream from the center of the P-box. Although the results for the non-coding strand in α-cells do not show a continuously protected region for nucleosome I compared to naked DNA, the region between the hypersensitive sites at position −188 and −46 is clearly protected (Fig. 5(b), lanes 9, 10 and 11). The sensitive site within the footprint including position −167 is approximately five double helical turns away from the center of nucleosome I.

The region upstream of the P-box in the *STE2* UAS was not mapped, but there is additional strong protection for both DNA strands downstream of nucleosome I, starting from the nuclease hypersensitive site at position −15. This footprint has been assigned to nucleosome II with its center roughly located at a site 60 bp downstream of the transcription origin. The map of the DNA from **a**-cells does not appear significantly different to naked DNA, with the possible exception of the region that was assigned to nucleosome II in α-cells (Fig. 5(a), lanes 5 and 6; Fig. 5(b), lanes 12 and 13). The locations of nucleosome I and II are summarized in Figure 6.

To analyze the structure of nucleosome I in greater detail, DNase I maps of the *STE2* UAS were made using whole cell lysates. DNase I preferentially attacks the sites along nucleosomal DNA where the minor groove is exposed on the surface (Simpson & Whitlock, 1976; Lutter, 1979). If a nucleosome is stably positioned in a rotational sense, DNase I cuts should occur with approximately a 10 bp periodicity corresponding to the twist and accessibility of the DNA double helix. The DNase I cutting sites within the region of nucleosome I in α-cell chromatin are significantly different from those in naked DNA, with both nuclease hypersensitive and protected sites being observed (Fig. 7, lanes 3 to 6). A 10 bp ladder typical of a nucleosome on limited DNase I cleavage is seen in the region of nucleosome I in α-cell chromatin, but not in naked DNA. From base −48 to −185, 11 of the 12 steps, including the upstream end of the ladder, can be seen. The first site at position −186 is only two bases away from the site seen in the MNase digestion experiment, and we therefore defined this position as the boundary of nucleosome I. The periodicity of DNase I cutting sites in α-cells for nucleosome I is consistent with a distinct rotational positioning of this nucleosome, while the MNase footprinting suggests that the translational position is also well defined.

The top strand of nucleosome I was also mapped by DNase I, but in contrast to *in vitro* DNase I mapping experiments of reconstituted nucleosomes, no repeating 10 bp ladder was observed on the other strand of this nucleosome. Similar results have been found *in vivo* for positioned nucleosomes in the URA3 gene within the minichromosome YRp TRURAP (F. Thoma, personal communication).

Analogous mapping experiments were performed for the *STE3* UAS in **a** and α-cells. A sequence 1500 bp in length were examined by indirect end-labeling, and the P′/Q-box region was analyzed by ligation-mediated PCR to obtain high resolution information. Although the experiments were repeated several times, footprints corresponding to well-positioned nucleosomes were not observed (results not shown). We note that this data does not exclude the presence of nucleosomes in this region, but may simply reflect a positional degeneracy.

(e) *DNase I maps of the* STE2 *TATA-element in* ***a*** *and α-cells*

A region of weak DNase I protection at the TATA-box of the *STE2* promoter between position −43 and −55 can be identified on the coding strand

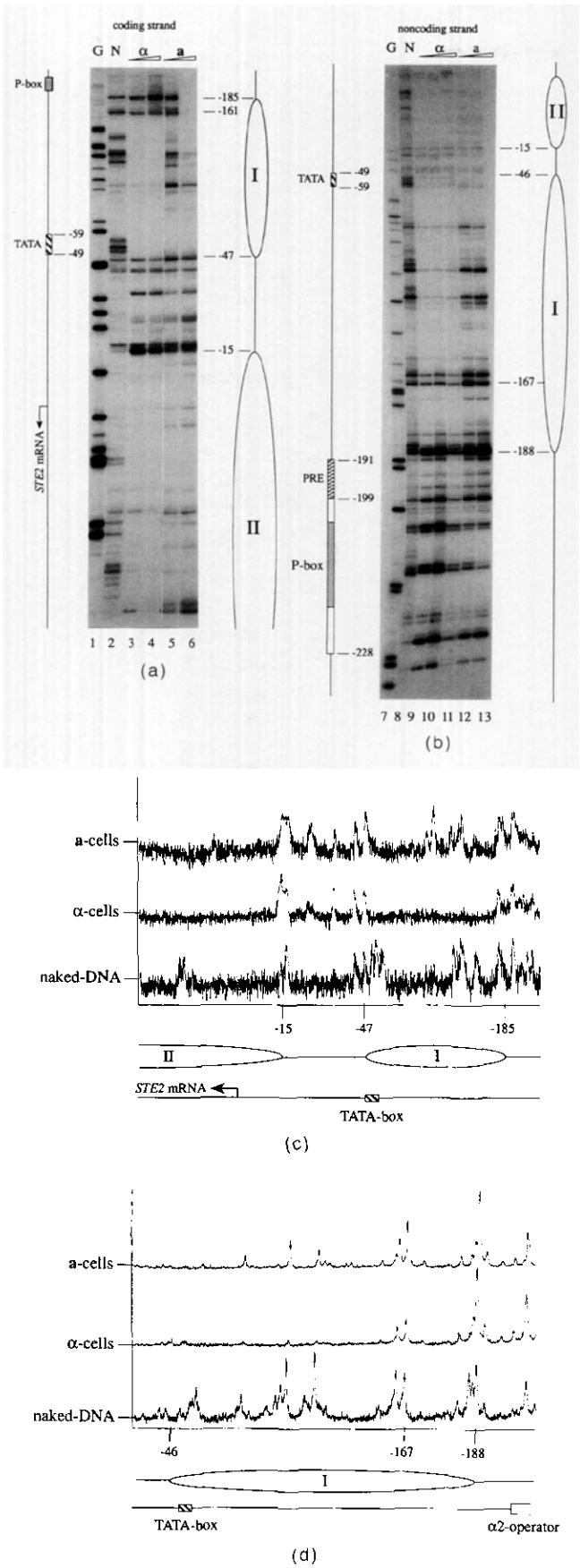

Figure 5. Genomic footprints of the *STE2* UAS and initiation site at high resolution in **a** and α-cells. Chromatin was cleaved with MNase in whole cell, followed by analysis of the *STE2* promoter using ligation-mediated PCR. (a) The map for the coding strand. For α-cells, digestion with 20 and 30 units enzyme/ml gives the pattern in lanes 3 and 4, and analogously for **a**-cells in lanes 5 and 6. (b) The map for the non-coding strand. For α-cells, digestion with 20, 30, 40 units enzyme/ml gives the pattern in lanes 9, 10 and 11, and analogously for **a**-cells with 20 and 30 units enzyme/ml in lanes 12 and 13. (a) and (b) A limited digestion of naked chromosomal DNA with MNase is shown in lanes 2 and 8, respectively (N), and with DMS modification at G bases in lanes 1 and 7, respectively (G). The boundaries of the nucleosomes relative to the initiation codon are indicated to the right. (c) Densitometric scan of (a) lane 5, **a**-cell, lane 3, α-cell, and lane 2, naked DNA. The locations of nucleosomes I (−185 and −47) and II (−15) are indicated. (d) Densitometric scan of (b): lane 12, **a**-cell, lane 9, α-cell, and lane 8, naked DNA. The locations of nucleosome I (−188 and −46) are indicated.

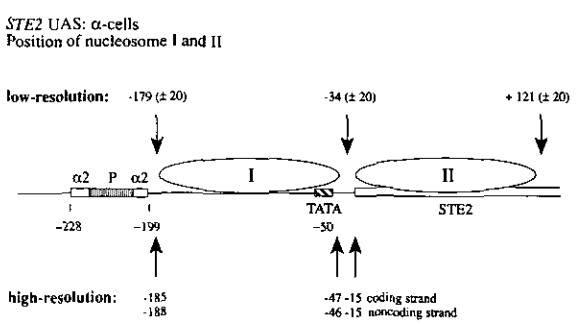

Figure 6. Nucleosome positions at the transcription initiation site of the *STE2* gene in α-cells. Nucleosome I and II boundaries determined from both low and high resolution chromatin maps made with MNase are indicated. The bases are numbered as for Fig. 1.

in **a**-cell chromatin (Fig. 8, lanes 5 and 6). This region of protection is followed by a strong nuclease hypersensitive site at position −42, which is seen neither in naked DNA nor in α-cell chromatin. The combination of weak protection and the strong enhancement of DNase I cutting pattern in this region provides evidence for the presence of a factor, probably the general transcription factor TFIID, bound to this element in **a**-cells. The protected region of approximately 13 bp corresponds to the 10 bp DNA-binding site proposed for the TATA-binding protein component of TFIID based on its crystal structure (Nikolov *et al.*, 1992). Additional protection is also observed for base −30 in **a**-cells but not in α-cells.

4. Discussion

To elucidate specific protein-DNA interactions that occur *in vivo*, and to understand their function in regulating gene specific transcription, we have mapped the structure of the 5′-regulatory regions of the **a**-specific *STE2* and the α-specific *STE3* genes in **a** and α-cells. Nucleotide-level resolution mapping was performed using a modified version of the ligation-mediated polymerase chain reaction procedure

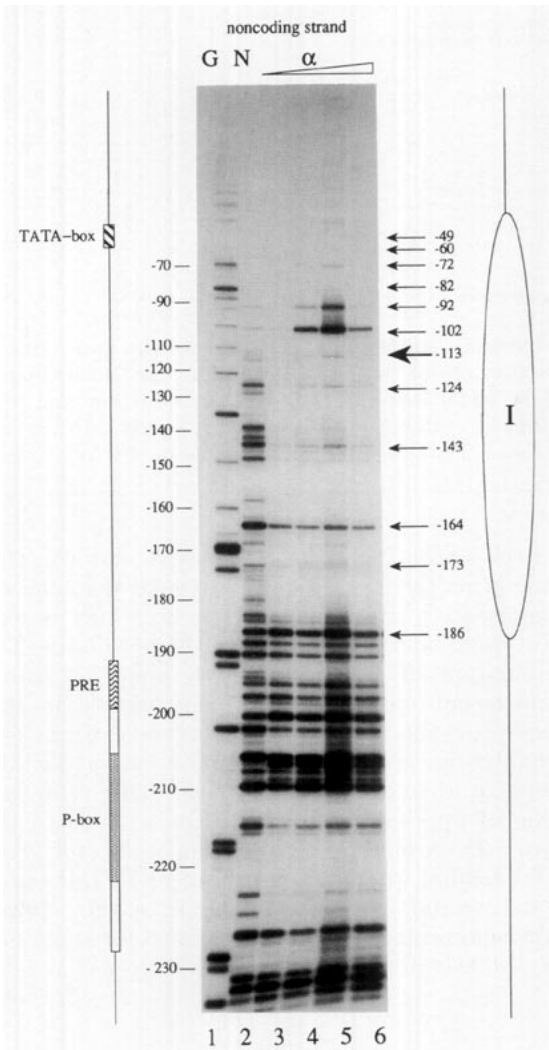

Figure 7. Genomic DNase I footprint of nucleosome I of the *STE2* gene in α-cells. Cleavage of the naked chromosomal DNA at G residues is shown in lane 1 (G), and with DNase I in lane 2 (N). Lanes 3 to 6 show the protection pattern in α-cells with 8, 10, 15 and 20 units enzyme/ml, respectively. The nuclease sensitive sites within nucleosome I, which form a 10 bp ladder, are indicated by arrows. The position of nucleosome I is shown on the right, and the P-box region and TATA-element are shown on the left. The bases are numbered as for Fig. 1.

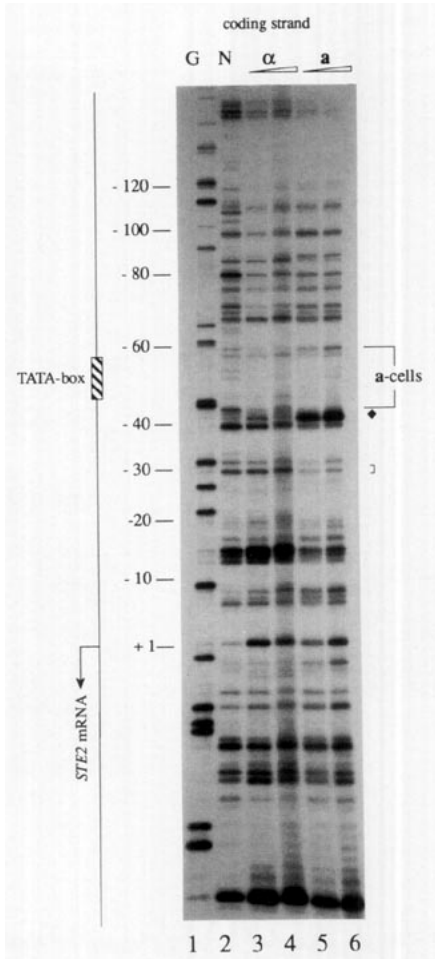

Figure 8. Genomic DNase I footprint of the TATA-box of the *STE2* gene in **a** and α-cells. The coding strand was analyzed. Cleavage of the naked chromosomal DNA at G residues is shown in lane 1 (G), and with DNase I in lane 2 (N). Lanes 3 and 4 show the protection pattern of the DNA from DNase I digestion in α-cells, lanes 5 and 6 show the protection pattern in **a**-cells. The region protected in **a**-cells is indicated by the square bracket. The bases are numbered as for Fig. 1.

of Mueller & Wold (1989). We treated whole yeast cells with DMS and spheroplasts with DNase I or micrococcal nuclease to obtain genomic footprints. Sequence specific interactions were detected by comparing the cleavage pattern of chromatin with the pattern observed for naked genomic DNA and in several cases with those from complexes prepared *in vitro*. The DNA sequences that include the binding sites of the transcription factors MCM1, MATα1, MATα2, STE12 and TFIID as assembled in chromatin are the focus of this study (Fig. 9).

As anticipated from previous *in vitro* experiments (Tan *et al.*, 1988), MCM1 binds to the 16 bp near-palindromic P-box of the *STE2* UAS in **a**-cells, within the α2 operator site. It is likely that MATα2 binds to the sequences of the operator site flanking the P-box in α-cells since the DMS protection pattern in α-cells extends on either side of the P-box protection observed in **a**-cells. No such extension was observed when DNase I was used, although details of the footprinting pattern do differ between **a** and α-cells. We attribute this negative result to possible rearrangement or degradation of the complexes during the additional time and steps required for the DNase I procedure. Alternatively, additional factors such as SSN6/TUP1 might modulate the binding of MCM1 and MATα2 to the UAS element and alter the pattern.

The STE12 protein is a component of the pheromone response pathway that is activated when either **a** or α-cells bind the pheromone from the opposite cell type. The STE12 binding site or PRE is immediately downstream of the P-box in the *STE2* UAS, and Errede & Ammerer (1989) have

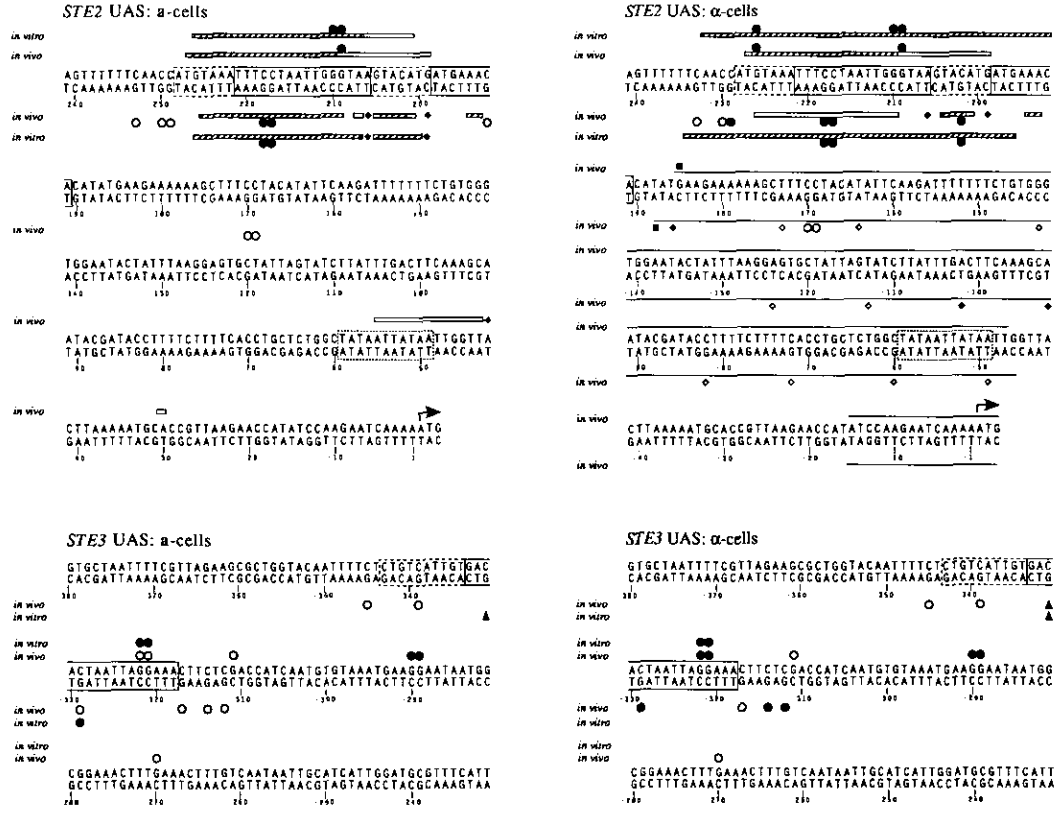

Figure 9. Summary of DMS, DNase I and micrococcal nuclease genomic footprinting data in **a** and α-cells. The upstream sequences are shown for the *STE2* UAS (Burkholder & Hartwell, 1985) with the P-box, PRE and TATA-box indicated, and for the *STE3* UAS (Bender & Sprague, 1987) with the P′/Q-box and TATA-box indicated. *In vitro* footprint data of the binary MCM1-*STE2* complex, the ternary MCM1-MATα2-*STE2* complex and the binary MCM1–*STE3* complex is also shown. Numbering is relative to the transcriptional start site. The keys to reactivity are as follows: ●, DMS strongly protected; ○, DMS partially protected; ▲, DMS hypersensitive; ▨, DNase I strongly protected; □, DNase I weakly protected; ◆, DNase I hypersensitive; ◇, DNase 10 bp ladder step; (—), MNase protection; ■, MNase hypersensitive.

shown by *in vitro* DNase I footprinting that **a**-cell extracts footprint the P-box and the PRE. The DMS and DNase I genomic footprints shown here reveal protection of the PRE in **a**-cells, consistent with STE12 binding to the PRE in this cell type. Although a similar DNase I genomic footprint is observed for the PRE in α-cells, significant protection against DMS methylation is not seen in α-cells. Therefore, we are unable to conclude with certainty whether or not STE12 binds to the PRE in α-cells.

The pattern of DMS protection of the *STE3* UAS in **a** and α-cells is more complicated. Results consistent with MCM1 binding to the P′-box in **a**-cells are obtained for the coding strand, but not for the non-coding strand, although *in vitro* footprinting shows a pattern of DMS protection and enhancement on both strands. In contrast, the methylation protection pattern of the *STE3* UAS in α-cells is consistent with the concerted binding of MCM1 and MATα1 observed *in vitro* using purified polypeptides. However, additional protection not detected *in vitro* can be seen in both cell types on the Q-box side distal to the P′-box and in the regions around −290 and −313. There may be additional factors that bind to these regions, although the significance of the putative binding sites around −290 and −313 to cell-type specific transcription is unclear since the 26 bp P′Q box has been shown to be both sufficient and necessary for α-specific regulation (Hwang-Shum *et al.*, 1991). The additional protection of the Q-box at −339 is of particular interest since the half of the Q-box distal to the P-box is conserved among several α-specific UAS elements and yet is not required for MATα1 to bind (S. Tan & T. Richmond, unpublished results) as was initially proposed. If additional factors do bind to this distal half of the Q-box, they may potentially modulate the binding of MCM1 to the P′ region. Such additional Q-box factors may account for the different results of binding MCM1 to α-specific UAS elements obtained depending on whether crude extracts or purified MCM1 are used in the *in vitro* binding experiments.

A combination of low and high resolution mapping experiments demonstrate that nucleosomes are translationally and rotationally well positioned on the transcriptionally repressed **a**-specific *STE2* gene in α-cells. The 10 bp repeating DNase I protection ladder establishes that nucleosome I is also precisely positioned rotationally. Micrococcal

nuclease was used at both high and low resolutions to map the translational positions of the nucleosomes in the *STE2* promoter, and the results indicate that nucleosome I is centered 96 bp downstream of the center of the P-box and 56 bp upstream of the TATA-box. This places the edge of nucleosome I 14 bp from the downstream edge of the MATα2 operator. In addition, the *STE2* TATA-box, the binding site for TFIID and the platform for the rest of the basal transcription apparatus, is protected in α-cells from both micrococcal nuclease and DNase I digestion by the final turns of nucleosome I. These results match similar studies performed on the promoters of two other **a**-specific genes, *STE6* and *BAR1*, which show precisely positioned nucleosomes 15 and 16 bp downstream from the edge of the MATα2 operator. In these studies, the TATA element is located near the dyad of the nucleosome. Such observations suggest that MATα2 mediated repression of these genes involves stable positioning of nucleosomes that cover the TATA element in the promoter. MATα2 may actually contact histone proteins since mutant strains having deletions in the amino terminus of histone H4 do not yield a nucleosome footprint on *STE6* (Roth *et al.*, 1992).

The *STE2* TATA-box is also protected from digestion by DNase I in **a**-cells but unlike the nucleosomal protection in α-cells, the protection is limited only to the TATA region. No positioned nucleosomes are observed for the promoter regions of the transcriptionally active *STE2* gene in **a**-cells, nor for the α-specific *STE3* gene in either **a** or α-cells. We presume that this protection in **a**-cells is due to TFIID binding to the TATA-box. The protection of the transcriptionally active *STE2* TATA-box in **a**-cells is also accompanied by a nuclease hypersensitive site immediately downstream of the TATA-box and this hypersensitive site is not observed in the transcriptionally repressed *STE2* gene in α-cells. A similar hypersensitive site near the TATA element of the **a**-specific *STE6* gene in α-cells was previously noted (Shimizu *et al.*, 1991). Other transcriptionally active genes may also contain such characteristic nuclease hypersensitive sites near the TATA-box.

These studies suggest that upstream activators and repressors might influence the expression of cell-type specific genes in the yeast *S. cerevisiae* via the organization of the chromatin structure. The presence of the repressor MATα2 is correlated with the precise positioning of nucleosomes downstream of the **a**-specific *STE2* and *STE6* UAS elements in α-cells. In both cases, a positioned nucleosome overlaps the TATA-box and may inhibit binding by the general transcription machinery to this site with the result that the **a**-specific genes are repressed in α-cells. In contrast, since MATα2 is not present in **a**-cells, there are no positioned nucleosomes to block accessibility of the general transcriptional machinery to the TATA-box, and therefore these **a**-specific genes are expressed in **a**-cells.

The importance of MCM1 or other protein cofactors to nucleosome positioning remains to be determined. MCM1 binds co-operatively with MATα2 to the MATα2 operator and is a corepressor of the **a**-specific genes in α-cells (Keleher *et al.*, 1992), but it is not known if MCM1 is required for the precise positioning of nucleosomes observed.

Successful application of the DMS, DNase I and MNase on whole-cells or spheroplasts provides us with detailed *in vivo* footprints for two transcriptional regulatory sites, the **a**-specific *STE2* and the α-specific *STE3* UAS. Our results demonstrate that different specific protein-DNA assemblies occur on these two UAS-elements in **a** and α-cells and suggest that the different architectures found for the promoter regions determine the transcriptional state of the genes. The *in vivo* DNA protection maps point specifically to complexes that can be constructed and studied *in vitro*.

We thank Y. Hunziker for DNA oligonucleotide synthesis and D. Sargent for help with densitometry. We are also grateful for advise about indirect end-labeling from M. Livingstone-Zachej and F. Thoma.

References

Ausubel, F. M., Brent, R., Kingston, R. E., Moore, D. D., Seidman, J. G. Smith, J. A. & Struhl, K. (1987). *Current Protocols in Molecular Biology*. John Wiley & Sons, New York.

Bender, A. & Sprague, G. F. Jr (1987). MATα1 protein, a yeast transcription activator, binds synergistically with a second protein to a set of cell-type-specific genes. *Cell*, **50**, 681–691.

Bruhn, L., Hwang-Shum, J.-J. & Sprague. G. F., Jr (1992). The N-terminal 96 residues of MCM1, a regulator of cell type-specific genes in *Saccharomyces cerevisiae*, are sufficient for DNA binding, transcription activation, and interaction with α1. *Mol. Cell. Biol.* **12**, 3563–3572.

Burkholder, A. C. & Hartwell, L. H. (1985). The yeast α-factor receptor: structural properties deduced from the sequence of the *STE2* gene. *Nucl. Acids Res.* **13**, 8463–8475.

Carlson, M., Osmond, B. C., Neigeborn, L. & Botstein, D. (1984). A suppresser of SNF1 mutations causes constitutive high-level invertase synthesis in yeast. *Genetics*, **107**, 19–32.

Church, G. M. & Gilbert, W. (1984). Genomic sequencing. *Proc. Nat. Acad. Sci., U.S.A.*, **81**, 1991–1995.

Dolan, J. W., Kirkman, C. & Fields, S. (1989). The yeast STE12 protein binds to the DNA sequence mediating pheromone induction. *Proc. Nat. Acad. Sci., U.S.A.*, **86**, 5703–5707.

Elble, R. & Tye, B. K. (1991). Both activation and repression of **a**-mating-specific genes in yeast require transcription factor MCM1. *Proc. Nat. Acad. Sci., U.S.A.*, **88**, 10966–10970.

Errede, B. & Ammerer, G. (1989). STE12, a protein involved in cell-type-specific transcription and signal transduction in yeast, is part of protein-DNA complexes. *Genes Develop.* **3**, 1349–1361.

Feinberg, A. P. and Vogelstein, B. (1983). A technique for radiolabeling DNA restriction endonuclease fragments to high specific activity. *Anal. Biochem.* **132**, 6–13

Hartig, A., Holly, J., Saari, G. & MacKay, V. L. (1986).

Multiple regulation of *STE2*, a mating-type-specific gene of *Saccharomyces cerevisiae*. *Mol. Cell. Biol.* **6**, 2106–2114.

Hayes, J. J. & Wolffe, A. P. (1992). The interaction of transcription factors with nucleosomal DNA. *BioEssays*, **14**, 597–603.

Herskowitz, I. (1988). Life cycle of the budding yeast *Saccharomyces crevisiae*. *Microbiol. Rev.* **52**, 536–553.

Herskowitz, I. (1989). A regulatory hierarchy for cell specialization in yeast. *Nature (London)*, **342**, 749–757.

Hwang-Shum, J. J., Hagen, D. C., Jarvis, E. E., Westhy, C. A. & Sprague, G. F., Jr (1991). Relative contributions of MCM1 and STE12 to transcriptional activation of **a** and α-specific genes from *Saccharomyces cerevisiae*. *Mol. Gen. Genet.* **227**, 197–204.

Jarvis, E. E., Hagen, D. C. & Sprague, G. F., Jr (1988). Identification of a DNA segment that is necessary and sufficient for α-specific control in *Saccharomyces cerevisiae*: implications for regulation of α-specific and **a**-specific genes. *Mol. Cell. Biol.* **8**, 309–320.

Johnson, A. D. & Herskowitz, I. (1985). A repressor (*MATα2* product) and its operator control expression of a set of cell type specific genes in yeast. *Cell*, **42**, 237–247.

Jones, E. W. (1991). Tackling the protease problem in *Saccharomyces cerevisiae*. *Methods Enzymol.* **194**, 428–453.

Keleher, C. A., Goutte, C. & Johnson, A. D. (1988). The yeast cell-type-specific repressor α2 acts co-operatively with a non-cell-type-specific protein. *Cell*, **50**, 143–146.

Keleher, C. A., Redd, M. J., Schultz, J., Carlson, M. & Johnson, D. (1992). Ssn6-Tup1 is a general repressor of transcription in yeast. *Cell*, **68**, 709–719.

Kronstad, J. W., Holly, J. A. & MacKay, V. L. (1987). A yeast operator overlaps an upstream activation site. *Cell*, **50**, 369–377.

Lutter, L. C. (1979). Precise location of DNase I cutting sites in the nucleosomal core determined by high resolution gel electrophoresis. *Nucl. Acids Res.* **6**, 41–56.

Maxam, A. M., & Gilbert, W. (1980). Sequencing end-labeling DNA with base-specific chemical cleavages. *Methods Enzymol.* **65**, 499–560.

Mueller, P. R. & Wold, B. (1989). *In vivo* footprinting of a muscle specific enhancer by ligation mediated PCR. *Science*, **246**, 280–286.

Nakayama, N., Miyajima, A. & Arai, K. (1985). Nucleotide sequences of *STE2* and *STE3*, cell type-specific sterile genes from *Saccharomyces cerevisiae*. *EMBO J.* **4**, 2643–2648.

Nikolov, D. B., Hu, S.-H., Lin, J., Gasch, A., Hoffmann, A., Horikoshi, M., Chua, N.-H., Roeder. R. G. & Burley, S. K. (1992). Crystal structure of TFIID TATA-box binding protein. *Nature (London)*, **360**, 40–46.

Norman, C., Runswick, M., Pollock, R. & Treisman, R. (1988). Isolation and properties of cDNA clones encoding SRF, a transcriptional factor that binds to the *c-fos* serum response element. *Cell*, **55**, 989–1003.

Passmore, S., Elble, R. & Tye, B. K. (1989). A protein involved in minichromosome maintenance in yeast binds a transcriptional enhancer conserved in eukaryotes. *Genes Develop.* **3**, 921–935.

Roth, S. Y., Shimizu, M. Johnson, L., Grunstein, M. & Simpson, R. T. (1992). Stable nucleosome positioning and complete repression by the yeast α2 repressor are disrupted by amino-terminal mutations in histone H4. *Genes. Develop.* **6**, 411–425.

Sambrook, J., Fritsch, E. F. & Maniatis. T. (1989). *Molecular Cloning: A Laboratory Manual* Cold Spring Harbor Laboratory Press, Cold Spring Harbor, NY.

Sanger, F., Nicklen, S. & Coulson, A. R. (1977). DNA Sequencing with chain-terminating inhibitors. *Proc. Nat. Acad. Sci., U.S.A.*, **74**, 5463–5467.

Schultz, J. & Carlson, M. (1987). Molecular analysis of SSN6, a gene functionally related to the SNF1 protein kinase of *Saccharomyces cerevisiae*. *Mol. Cell. Biol.* **7**, 3637–3645.

Shimizu, M., Sharon Y. R., Szent-Gyorgy, C. & Simpson, R. T. (1991). Nucleosomes are positioned with base-pair precision adjacent to the α2 operator in *Saccharomyces cerevisiae*. *EMBO J.* **10**, 3033–3041.

Simpson, R. T. (1990). Nucleosome positioning can affect the function of a *cis*-acting DNA element *in vivo*. *Nature (London)*, **343**, 387–389.

Simpson, R. T. (1991). Nucleosome positioning: occurrence, mechanisms, and functional consequences. *Progr. Nucl. Acid Res. Mol. Biol.* **40**,143–184.

Simpson, R. T. & Whitlock, J. P. (1976). Mapping DNase I-susceptible sites in nucleosomes labeled at the 5′ ends. *Cell*, **9**, 347–353.

Sprague, G. F., Jr (1990). Combinatorial associations of regulatory proteins and the control of cell type in yeast. *Advan. Genet.* **27**, 33–67.

Sprague, G. F., Jr, Jensen, R. & Herskowitz, I. (1983). Control of yeast cell type by the mating type locus: positive regulation of the α-specific *STE3* gene by the MATα1 product. *Cell*, **32**, 409–415.

Straka, C. & Hörz, W. (1991). A functional role for nucleosomes in the repression of a yeast promoter. *EMBO J.* **10**, 361–368.

Strathern, J., Hicks, J. & Herskowitz, I. (1981). Control of cell type in yeast by mating type locus: the α1-α2 hypothesis. *J. Mol. Biol.* **147**, 357–372.

Tan, S. & Richmond, T. J. (1990). DNA binding-induced conformational change of the yeast transcriptional activator PRTF. *Cell*, **62**, 367–377.

Tan, S., Ammerer, G. & Richmond, T. J. (1988). Interactions of purified transcription factors: binding of yeast MATα1 and PRTF to cell type-specific, upstream activating sequences. *EMBO J.* **7**, 4255–4264.

Thoma, F., Bergmann, L. W. & Simpson, R. T. (1984). Nuclease digestion of circular TRP1ARS1 chromatin reveals positioned nucleosomes separated by nuclease sensitive regions. *J. Mol. Biol.* **177**, 715–733.

Treisman, R. (1985). Transient accumulation of *c-fos* RNA following serum stimulation requires a conserved 5′-element and *c-fos* 3′ sequences. *Cell*, **42**, 889–902.

Treisman, R. (1986). Identification of a protein-binding site that mediates transcriptional response of the *c-fos* gene to serum response. *Cell*, **46**, 567–574.

Van Arsdell, S. W., Stetler, G. L. and Thorner, J. (1987). The yeast repeated element sigma contains a hormone-inducible promotor. *Mol. Cell. Biol.* **7**, 749–759.

Wahl. G. M., Berger, S. L. & Kimmel, A. R. (1987). Molecular hybridization of immobilized nucleic acids: theoretical concepts and practical considerations. *Methods Enzymol.* **152**, 399–407.

Edited by M. Yaniv